Effects of HCl hydrolyzed cellulose nanocrystals from waste papers on the Hydroxypropyl methylcellulose/Cationic Starch biofilms

khashayar vaezi (ka.vaezi@stu.sanru.ac.ir)
Sari Agricultural Sciences and Natural Resources University https://orcid.org/0000-0002-3084-4074
Ghasem Asadpour
Sari Agricultural Sciences and Natural Resources University

Research Article

Keywords: Waste Paper, Nanocrystalline Cellulose, Hydroxypropyl methylcellulose, Biopolymers, Bionanocomposite Films

Posted Date: January 13th, 2022

DOI: https://doi.org/10.21203/rs.3.rs-674427/v1

Version of Record: A version of this preprint was published at Waste and Biomass Valorization on January 12th, 2022. See the published version at https://doi.org/10.1007/s12649-021-01651-3.

Abstract

ABSTRACT

The study reports on the preparation of nanocrystalline cellulose from waste papers (WPNCC), as an environmental friendly approach of source material and investigation of their effects on the morphological, mechanical and barrier properties of the Hydroxypropyl methylcellulose/Cationic starch (HPMC/CS) nanocomposites. HCl hydrolysis followed by alkali treatment and deinking of the fibers resulted in the production of WPNCC. The TEM results confirmed the rod like shape of WPNCC; the average diameter was 22± 7 nanometers and the length was 125± 25 nanometers. The hydrolysis yield was 65% with high crystallinity index of 79.6%. The results of X-ray diffraction confirmed the successfully production of WPNCC and their effective presence in the HPMC/CS matrix. The homogeneity of WPNCC dispersion in the polymer matrix was approved by FESEM analysis. The WPNCC also did not affect the nanocomposites optical clarity. The optimum amount of 9 wt% WPNCC, showed the highest barrier, mechanical and biodegradablility properties.

Statement Of Novelty

In this study we worked on the production of cellulose nanocrystals from Waste Papers (as a recycled source to make an added value). This process (Waste Papers to NCC) has done by HCl hydrolysis for the first time in order to have improved particles sizes and improved properties. Then we studied the effects of these produced nanocrystals on the fundamental properties and biodegradability of the Hydroxypropyl methylcellulose/Cationic Starch nanocomposites for the first time.

1. Introduction

Environmental impacts have reached a critical stage, causing serious consequences to the natural environment all over the world. This is due to the industrial development of great world powers, developing countries, and even third world countries [1]. In recent years, solid wastes generated by different industrial, mining, domestic and agricultural activities have raised serious environment issues [2]. Among all solid wastes, huge amount of waste paper which comes from office plays an important role in damaging the ecology of the earth. It is usually underutilized and finally achieves to burning or slow biodegradation [3]. As reported, recycling of one ton of waste paper can save approximately 3 tons of wood and 27 tons of water [4], which has great environmental and economic benefits. Therefore, how to make this paper from waste to wealth and use it in new approaches, i.e. recycling of office waste paper (OWP), have become a meaningful and challenging work. In last years, while the demand of packaging papers is increasing continuously, the use of newsprint and some other graphic papers is decreasing. For example the production of packaging papers in Europe increased 7.2% in the last five years, while newsprint production decreased in 28.3% (CEPI 2015). This fact supposes huge challenges for the newsprint mills in order to maintain their competitiveness. As a consequence some companies have shut down production lines and others are looking for other market niches by developing new products and

high added value products [5]. It must be noted that the reuse or second stage utilization of papers is further a pressure on environment by making of greenhouse gases on burning during anthropological activities. Among all solid wastes produced, annually several million tons of paper is produced and utilized worldwide which gives rise to a huge amount of wastepaper [4]. Huge amount of waste paper, which comes from offices, is currently underutilized and finally achieve to burning or slow biodegradation. Also, the waste paper is difficult to recycle because the number of times paper can be reprocessed by paper industry is limited due to the shortening of the fiber length and the resulting reduction in tensile strength. Thus, the loss of paper making properties causes it to occupy 30– 40% of landfill sites in developed countries [2]. In accession to this, the cellulosic rich fibers, left over from the process of papermaking, are discharged with the wastewater in amounts of several thousand tons a year [4]. Feeble mechanical strength of waste paper has some drawbacks to use in the paper industry. In this sense, the production of nanocellulose can be a very promising alternative. Cellulose, a type of polysaccharides, which is in abundant consists of both crystalline phase and amorphous region. The removal of the amorphous region by acid hydrolysis results in the formation of highly ordered (crystalline) structure, the cellulose nanocrystal. Reviews in the field of cellulosic nanomaterial has been reported by [6–9]. The geometry and characteristic of cellulose nanocrystals made it an ideal material for various potential applications such as polymer electrolyte [10], gel nanomaterial [11], polymer nanocomposite membrane [12], and biomedical [13]. Preparation of cellulose nanocrystals can be achieved through isolation of cellulose particles from many sources such as Ramie [14], Bacteria [15], Wood pulps [16], Mengkuang leaves [17], and Cotton [18]. As is known to all, waste paper is rich in cellulose with small amounts of hemicellulose. If it would be effectively utilized, high value utilization could be achieved. Furthermore, it is of practical significance to reduce the influence of impurities like lignin, filler, ink, and ash, improving the utilization of waste paper fiber and bring higher economic benefits. Identical with cellulose, cellulose nanocrystal is also a linear polymer composed of structural units of the β-D-glucosamine linked by 1, 4-β glycosides, whose chemical formula is ($C_6H_{10}O_5$). Due to its unique characters, such as excellent mechanical properties, unique optical properties (liquid crystal), special rheological behavior, better biocompatibility and high reactive activity, NCC have a wide application value, attracting much attention in various fields [19, 20]. On the other hand, in these years, the application of eco-friendly biodegradable polymers increases to avoid uses of nonbiodegradable synthetic polymers from petroleum source which give rise to environmental problems [21]. But Eco-Friendly biodegradable polymers such as methylcellulose, hydroxypropyl methylcellulose, starch, lignin, cellulose acetate, polyvinyl alcohol (PVA) and polyester have lower mechanical, barrier, water resistance properties and thermal properties compare to synthetic polymers. Therefore, to replace nonbiodegradable petrochemical synthetic polymers by biodegradable polymers, properties of biodegradable polymers are to be improved by several methods such as blending with synthetic polymers [22] or natural polymers [21] or by adding nanofillers [23, 24] and also by crosslinking [25]. Hydroxypropyl methylcellulose (HPMC) is one of the cellulose ethers which is the most commonly used. It is approved for food uses by the FDA (21 CFR 172.874) and the EU (EC, 1995) and it is used in the food industry as an emulsifier, protective colloid, stabilizer, suspending agent, thickener, or film former. The films obtained from HPMC are resistant to oils and fats, flexible, transparent, odorless, and tasteless but tend to have moderate strength [26]. Indeed the

use of agro-industrial biodegradable polymers has been limited because of problems related to performance such as brittleness and poor gas and moisture barrier. The application of nanotechnology by developing polymer nanocomposite films with the addition of fillers in the nanometric range or blending with other polymers may open new possibilities for improving these mechanical and barrier properties [26]. In this work, we considered Cationic Starch (CS) as a blending polymer with HPMC matrix. CS is preferred because the positive charge that has been introduced onto the starch molecule chain tends to form an electrostatic bond with negative charge sites on the fillers and polymers [24]. CS is prepared by the starch treatment with cationizing reagents such as 2, 3-(epoxypropyl) trimethylammonium chloride and 2-diethylaminoethyl chloride [27]. Because of the renewable nature and the environmentally friendly character and low cost, CS is commonly applied in the paper industry [28, 29]. To the best of our knowledge, no study has been reported on the effects of Waste Papers nanocrystalline cellulose (WPNCC) particles on the properties of HPMC/CS nanocomposites. The present study was aimed to investigate the production of NCC nanoparticles from waste papers by HCl hydrolysis for the first time and the dispersion of these nanoparticles with different percentages in the first time blended HPMC/CS matrix and their effects on the nanocomposites morphology, mechanical and barrier properties.

2. Materials And Methods

2.1. Materials

Office waste papers were collected from sari agricultural sciences and natural resources university laboratory (Sari, Mazandaran, Iran). Glycerol was purchased from Merck Company (Germany). HCl (Merck, Germany) with 37 wt% concentration was applied in order to acidic hydrolysis of alpha cellulose of waste papers in order to obtain NCC. HPMC (Sigma-Aldrich Germany) and CS with water content, pH and substitution's degree of 18± 0.19%, 6.9 and 0.035, respectively (from Mazandaran wood and paper mill Sari, Mazandaran, Iran), were used as biopolymer matrices. NaOH was used in order to produce 85% RH. $CaCl_2$ was applied as desiccant. H_2O_2 and NaOH were used for deinking and purification of papers pulp. All these agents were attained from Sigma-Aldrich (Germany) and applied without further modification.

2.2. Deinking and defibering of waste papers

The waste papers were collected from our laboratory and shredded into pieces of 15 mm× 4 mm by paper shredder. After that the solution of 2 wt% H_2O_2 and 2 wt% NaOH and 1000 milliliters of distilled water was made and blended with glass rod in order to produce deinking agents. The prepared deinking agents and paper pieces were added into the laboratory repulper and soaked for about half an hour. Afterwards, the repulper started to defibration at the speed of 3000 rpm and pulp concentration of 10%, for approximately 30 min. In the cooperation of chemical agents and mechanical forces ink fell off the waste papers and defibered papers was obtained. Subsequently, defibered papers were washed for several times through a fine-mesh for the purpose of removing the ink and impurities from the waste papers pulp. Finally, the

obtained pulp was dried in the furnace at 80°C for 24 h and smashed with the high-speed universal pulverizer (10000 rpm) for 10-30 seconds to obtained fine deinked pulp fibres, since the mechanical treatment resulted in disintegration of the cellulose structure into microcrystalline cellulose particles. The particles sizes before and after pulverizing were approximately obtained, 710- 840 µm and 25- 37 µm, respectively (by mesh sieving).

2.3. Preparation of WPNCC

Alkaline treatment was performed to purify cellulose by removing other constituents present in the fibers. This treatment was carried out by mechanically agitating the fibers into a NaOH solution (2 wt%) at room temperature and at constant speed for a period of 12 h. After the base treatment, the fibers were filtered washed with distilled water until a neutral pH was achieved and all of the alkali solution was completely removed. Fibers hydrolysis was carried out by mixing the fibers with a 3 molar HCl solution (40 mL per 1 g of cellulose fibers) at 100 ◦C for 180 min, with continuous magnetic stirring. The suspension obtained after hydrolysis was washed with distilled water until neutrality by successive centrifugations (around five times) of 15 min at 6000 rpm. The supernatant was collected and dialyzed against deionized water for 4– 5 days to remove the remaining acid and other chemicals (dialysis tube from Spectrum Laboratories Inc., cutoff molecular weight 12000– 14000). Finally the dialyzed suspension was dispersed and treated using a sonicator for 30 seconds (Qsonica- q700- USA, power: 7W). The CN dispersion was treated with a drop of chloroform to prevent bacterial growth and then stored in the fridge [30]. The final suspension was freeze dried (Vacuum freeze dryer with 1 kW power) to the powder for the further steps of the research and had a concentration of 3%.

2.4. Film Preparation

Nanocomposite films was produced by mixing HPMC (3 g), Cationic Starch (2 g), glycerol (30% based on dry weight of mixed HPMC/CS matrices), distilled water, and specified amounts of NCC suspension (3, 5, 7, 9, 11 wt%) based on dry weight of mixed HPMC/CS matrices. First of all, 3 g of (HPMC) and 2 g of (CS) were blended with 1.5 mL glycerol (30 mL/100 g HPMC/CS) and distilled water (100 mL) at 25°C for 5 min. This solution was heated at 85°C for 10 min, and was stirred with the speed of 500 rpm. Also, a specified contents of the WPNCC (3 wt%, 5 wt%,7 wt%, 9 wt% and 11 wt%) were diffused in distilled water separately and were sonicated (ultrasonic bath) for 30 min at 25°C. Then the WPNCC suspension were added to HPMC/CS solution slowly with severe stirring (1000 rpm, 5 min) in order to have a good dispersal and then sonicated at (40 KHz, 100 W, 30 min). In order to eliminate all air bubbles from suspension, a vacuum with a rotational pump was used. After that, 25 mL of suspension was transferred into a polystyrene tray to make nanocomposites with 0.08± 0.01mm thickness (measured with Mitutoyo digimatic Indicator Type ID-110E; Mitutoyo Manufacturing Co. Ltd., Tokyo, Japan with the resolution of 1 µm) and then it was oven-dried at 55°C for 16 h to cast the films [24]. The obtained nanocomposites were detached from the tray and then transferred into a desiccator at 25°C. It contained saturated solution of calcium nitrite at 20– 25°C to ensure a 55% relative humidity for 48 h before characterization. Pure HPMC/CS film without nano reinforcement was used as a control sample.

2.5. WPNCC characterization

2.5.1. Yield of WPNCC

Yield of WPNCC was calculated by equation below:

$$\text{Process Yield (\%)} = \frac{(m_1 - m_2) \cdot V_1}{m_3 \cdot V_2} \times 100 \quad (1)$$

Where, m_1 is the mass of freeze-dried sample and container (g), m_2 is the mass of container (g), m_3 is the mass of pure cellulose (deinked and defibered waste papers) (g) and V_1 and V_2 are total volume of WPNCC suspension and WPNCC suspension that was freeze dried (ml), respectively.

2.5.2. X-Ray diffraction (XRD) and Crystallinity index

XRD spectrums was accomplished in the span of 2θ = 1°- 80°. The step increment was 2θ = 0.05° in a D8 Discover X-ray Diffractometer (PW1730, Philips, Netherlands). The X-ray source was Cu Kα (λ = 1.5406 Å). The generator's voltage was 40 kV and the electrical current was 30 mA. The scans were done with the speed of 1°/min. To find the crystallite' diameter (D) of the nanoparticles of NCC, the Debye-Scherrer equation can be used:

$$D = \frac{0.9(\lambda)}{\beta \cos \theta} \quad (2)$$

In this equation, λ represents the X-ray's wavelength, θ represents the diffraction's angle and β is the peaks full width at half the maximum intensity of the diffraction line. The Segal's equation [31] was applied to calculate the Crystallinity index of the WPNCC:

$$\textit{Crystallinity index} = \frac{I_{002} - I_{Amorph}}{I_{002}} \times 100 \quad (3)$$

In which, I_{002} is the maximum intensity of the (002) plane in 2θ = 22.5^o and I_{Amorph} represents the diffraction intensity at 2θ = 18^o.

2.5.3. Transmission electron microscope (TEM) characterization of WPNCC

In order to analyze the WPNCC's length and shape, TEM or transmission electron microscopy was applied with a Philips EM208S 100KV microscope. Prior to using TEM, the WPNCC suspension was ultrasound dispersed evenly.

2.6. Characterization of the bionanocompoites

2.6.1. Field Emission Scanning Electron Microscopy (FESEM)

Using the FE-SEM microscope (Tescan-Mira3), the surface morphology of the nanocomposites was investigated. Initially the samples were put in the temperature of 25^{o}C near silica gel. The next step was mounting the samples on bronze stubs and coating them with gold plasma. The observation was done by the acceleration voltage of 20 kV.

2.6.2. X-Ray diffraction (XRD)

XRD spectrums was done in the span of 2θ = 1° and 80°. The step increment was 2θ = 0.05° in a D8 Discover X-ray Diffractometer (PW1730, Philips). The x-ray's source was Cu Kα (λ = 1.5406 Å). The generator's voltage was 40 kV. The electrical current was 30 mA. The scans were done at the speed of 1°/min.

2.6.3. Fourier transform infrared spectroscopy (FTIR)

This analysis was accomplished using a (Shimadzu 4100, Thermo Nicolet) spectrophotometer which had the resolution of 2 cm^{-1}. Its scans was in the span of 4000 cm^{-1} to 400 cm^{-1}.

2.6.4. UV–Vis spectroscopy

A Shimadzu UV-160A UV-Vis Recording Spectrophotometer was applied to record the nanocomposite films' transmission spectrums from 200 to 700 nm.

2.6.5. Water vapor permeability

The WVP test was accomplished in accordance with the ASTM method of 15.09:E96. The specimens were attached on the cells which consisted 25 grams of calcium chloride for achieving a 0% RH condition. At first, the cells were weighed and then were moved to a proper container with 60% RH at 25 ^{o}C for 24 hours. After that, the water vapor content was identified from the cell's weight gain. The weighing of cells for samples was performed after 24 hours. The WVP is calculated pursuant to the composed Fick and Henry's laws for gas dissemination via specimens:

$$wvp = \frac{x\Delta w}{A\Delta P} \quad (4)$$

Where Δw is the increased weight of the cell (g) after 24 h, A is the area of exposed film (31.67 ×10^{-4} m^2), x is the thickness of samples (mm) and ΔP is the differential water vapor pressure through the sample (ΔP = 3.282 kPa at 25 ^{o}C). Water vapor permeability is expressed in g mm/m^2 day kpa.

2.6.6. Films solubility

Weighing and drying of the nanocomposite films was done for 24 hours at the temperature of 105 ^{o}C. Weighing of the films was done after they had been dried (W_0) and they were then moved to 75 milliliters tubes which consisted 25 milliliters of distillated water. The tubes were shacked occasional for 24 h at 25 ^{o}C. Undissolved film was dried in an oven at 105 ^{o}C for 24 h after removal of distilled water. The residue

was weighed and named as W_f. The water solubility (WS) of the nanocomposites was calculated pursuant to following equation:

$$ws = \frac{w_0 - w_f}{w_0} \times 100 \quad (5)$$

2.6.7. Moisture Absorption

The process of absorbing the humidity of the HPMC/CS based nanocomposites was done as follows. First they were made into little pieces and then the drying started until the weights of the samples did not change. This was done using an oven with the temperature of 60 ^{o}C with the purpose of eliminating the humidity. Then the weighting of the samples was immediately done (W_i). The films were moved to a desiccator which had the constant humidity of 75% and contained a saturated NaCl solution (ASTM E 104– 85). After that, the weighing of the films was done after 24 hours (W_f). The equation for calculating absorption amount of the samples [32]:

$$Moistureabsorption(\%) = \frac{w_f - w_i}{w_i} \times 100 \quad (6)$$

2.6.8. Mechanical properties

In order to specify the mechanical characteristics of the HPMC/CS film and its nanocomposites, (ASTM D882- 95a) standard and (SANTAM STM-20-Iran) machine were used. The test was done with specimen's length of 55 millimeters and the width of 15 millimeters at the machine cross-head speed of 5 mm/min at the room temperature.

2.6.9. Oxygen permeability

The evaluation of Oxygen transmission rate (OTR) [cm^3 (m^2 d^1)] of the samples was done using an Oxygen permeation device (OXTRAN 2/21, M CON, USA). This evaluation was for circular samples with 50 cubic meters of surface area. It was done at the temperature of 25 ^{o}C and RH of 75% according to the procedure of ASTM F1927- 07 (2007). Samples were closed among two chambers (each one with two channels), the lower one filled with O_2 at a steady flow rate of (20 mL min^{-1}) to hold the pressure stable in that section. The other channel was filled with nitrogen carrier gas (0.98 part of nitrogen and 0.02 part of hydrogen), at steady flow rate of (10 mL min^{-1}). A colorimetric sensor evaluated the content of oxygen passed through the film into the carrier gas. The samples permeance (PO_2) was evaluated according to following Equation. This equation was used for evaluating the samples' permeance (PO_2):

$$PO_2 = \frac{OTR}{P} \quad (7)$$

In which:

PO_2 represents the samples' permeability [$cm^3/(m^2\ d^1\ Pa^1)$]. The oxygen transmission rate [$cm^3\ m^{-2}\ d^{-1}$] is presented as OTR; and the sectional pressure of oxygen is presented as p, which is the mol fraction of oxygen multiplied by the total pressure (nominally, one atmosphere) in the test gas side of the dissemination cell. The carrier gas side has the sectional pressure of 0 for Oxygen. This equation was used to calculate the oxygen's permeability coefficient ($P'O_2$):

$$P'O_2 = PO_2 \times t \quad (8)$$

In which:

$P'O_2$ represents the Oxygen's permeation coefficient [$cm^3/(m^1\ d^1\ Pa^1)$]. t represents the samples' mean thickness [mm].

2.6.10. Disintegrability in composting of HPMC/CS film and its nanocomposites

The disintegration test was applied with the purpose of evaluating the disintegrability of the neat HPMC/CS film and its nanocomposites. This evaluation was for the compost productions and was according to the ISO- 20200. A specified amount of compost was mixed with the synthetic bio-waste which was provided with specified content of sugar, oil, starch, sawdust and urea. The substrate water amount was 55 wt% and the aerobic status was stabilized by mixing it gently. All specimens were weighed and buried at 5– 7 cm depth in perforated boxes containing the provided mixture and incubated at 58°C. The samples were recovered by tweezer at various periods, cleaned with distilled water dried in an oven at 40°C for 24 h and reweighed. Disintegrability of the samples was obtained by normalizing the sample weight, at different stages of incubation, to the initial ones [33].

2.6.11. Statistical analysis

In order to analyze the samples, it was done in three time with complete randomizing of the experimental design. In order to randomize, (ANOVA) or analyzing of variance was applied in SPSS software (V. 16). To find the discrepancies between mean values of samples properties, the Duncan's multiple range test ($p \leq 0.05$) was applied.

3. Results And Discussion

3.1. Morphological characterizations of the WPNCC

The yield of nanocrystals obtained is considered to be an important issue related to the production of WPNCC [34]. Wang et al, stated that two key processes dictate the yield of NCC, the first being depolymerization of cellulose under low-severity conditions, *e.g.*: acid concentrations of <58 wt%, and the second being degradation of NCCs at very high-severity conditions (acid concentrations of ≥ 64 wt%)

[35]. (Table. 1) lists the comparison of the values of yield, length and crystallinity index of the cellulose nanocrystals obtained in the present study with the earlier reported values these three characteristics of NCC by various researchers using different types of natural cellulose raw materials. The yield obtained in the present study was found to be 65 wt%. It can be seen that the yield value obtained in this research is similar to many of the reported values. This is due to removing the impure parts in pretreatment which was beneficial to the acid's accessibility to cellulose. Comparing the results of this research with the others [36] (54.6%), who provided the NCC from recycled newsprint shows a slight improvement. Moreover, this has been showed that substances with inferior qualifications have the potential to be applied in producing NCC and their hydrolysis yield is comparable to the ones that are provided by Wang et al, who applied a bleached Kraft eucalyptus pulp and got to 58.7% [37]. The results published by Karim et al, showed that the crystallinity provided with sulfuric acid treatment is not as high as HCl, because HCl is a weaker acid with lower K_a value, which dissociated in water sparingly [38]. After using this method, the hydrochloric acid which penetrated in the cellulose's inner layer caused the hydrolysis of the amorphous regions of cellulose chain, meanwhile the crystalline parts had higher resistance because of their strong hydrogen bonds. As the process was progressing, the cellulose's glycosidic bonds broke which caused the formation of nanoparticles. (Fig. 1) shows TEM images of WPNCC. In order to accurately determine the diameter and length of WPNCC, analysis of TEM is necessary, because of the irreversible reunion of hydrogen bonds between WPNCC in the drying process. The average diameter of the rod-shaped nanocrystals was 22± 7 nm and the length was 125± 25 nm. It is an approved fact that ultrasonic treatment, the concentration of acid and the type of precursors, can be effective factors in forming WPNCC. The evaporation of water can be considered one of the causes of the aggregation in the WPNCC, the other cause is that the cellulose nanoparticle has a very small size and their high specific surface area leads to them being stacked on each other because of the van der Waals forces [39]. It is shown in (Fig. 2) that the produced WPNCC presents three peaks at $2\theta = 18.3^{o}$, $2\theta = 22.6^{o}$ and $2\theta = 34.5^{o}$ which were assigned to cellulose I [30]. The crystallinity index of the produced WPNCC was 79.6% and this is higher than reported by Ley et al. [40] for sulfuric acid hydrolysis of office waste papers (74.1%). The nanocrystals which had the HCl treatment showed higher crystallinity because the cellulose's amorphous parts were removed. During hydrolysis process, hydronium ions had influence over the more available amorphous regions of cellulose and split the glycosidic bonds, which led to creation of individual crystallites. Acid hydrolysis of cellulose caused bond cleavage, i.e., hydrolytic cleavage of glycosidic bonds between two anhydroglucose units. This action was counteracted by rearrangement of the tangling chain ends, which was favoured by release of internal strain. Thus the amorphous portion got dissolved by the acid hydrolysis, leaving behind the crystalline regions, and led to the higher crystallinity of the resultant cellulose nanocrystals [40].

3.2. Morphological characterizations of the bio nanocomposites

(Fig. 2) shows the XRD patterns of HPMC, CS, WPNCC, and their nanocomposite films. The XRD pattern of NCC, revealed diffraction peaks at $2\theta = 18.3^{o}$, $2\theta = 22.6^{o}$, and $2\theta = 34.5^{o}$ related to (002) lattice planes.

It is a characteristic of the structure of cellulose I [30]. HPMC showed a main diffraction peak at 2θ = 20.9∘, which corresponds to the diffraction peak of cellulose crystal planes (002). The diffraction peaks of HPMC are very broad, which indicated their semi-crystalline nature. Furthermore, HPMC possesses much smaller crystallite size, which is also indicated its amorphous nature. It is obvious from (Fig. 2) that CS has three sharp peaks at $2\theta = 17.3^{o}$, $2\theta = 19.5^{o}$, and $2\theta = 24.1^{o}$ that are related to its crystalline structure [27]. As can be seen in (Fig. 2), there is no sharp peak in the nanocomposites and it can be concluded that the shear and temperature status during gelatinization were sufficient to melt the most crystallites of HPMC and CS. In the lower concentration of nanocrystals (3 wt%), the diffusion of the nanoparticles was good might be due to the strong polar interactions between the HPMC/CS chains hydroxyl groups and nanocrystals [27]. The changes observed in the diffraction pattern in the HPMC/CS/WPNCC11% can be attributed to the presence of cellulose-I in WPNCC, which also confirms the existence of high concentration WPNCC in the HPMC/CS matrix [46]. As can be seen, in the HPMC/CS/WPNCC11% nanocomposite, the intensity of the diffraction peaks increased in comparison with HPMC/CS/WPNCC3% nanocomposite. This clearly indicated that the addition of high concentration WPNCC can affect the crystalline nature of HPMC/CS nanocomposite. Cellulose nanocrystals reinforcement can improve functional properties of the composite films, but nanoparticles must be well dispersed to achieve any benefit.

The FE-SEM images of HPMC/CS nanocomposites with different percentages of cellulose nanocrystals are shown in (Fig. 3). As can be seen in (Fig. 3a), the surfaces of the neat HPMC/CS film was smooth with no cracks and roughness. With addition of WPNCC at contents of (3 wt%, 5 wt%, and 7%), we can see the cellulose nanocrystals are well dispersed in the matrix of biopolymer with no agglomeration (Fig. 3b, c, d). It illustrated a smooth surface and no cracks as envisaged for a homogeneous substance. No bubbles or roughness emerged owing to the loading of WPNCC. This shows that WPNCC were dispersed homogenously within the HPMC/CS matrix, eventuating in a high contact area with polymeric chains, and thus made a stronger interaction and coherence on the interfaces of WPNCC and macromolecular chains of HPMC/CS polymer [27]. The nanocomposite contained 9 wt% of WPNCC showed some cracks and roughness because of increment of WPNCC contents (Fig. 3e). However, the less homogeneous and rough surface with more cracks was seen when the concentration of WPNCC enhanced to 11 wt% (Fig. 3f). It could be due to the agglomeration of WPNCC in the HPMC/CS matrix at high concentration [47]. The good dispersion of WPNCC in the HPMC/CS nanocomposite was associated with its effectiveness in improving the properties of nanocomposites. These results were a good indication of the excellent compatibility between the components of the nanocomposite films that resulted in highly homogeneous materials and smooth surface films. The smaller scale of the WPNCC is shown inside the HPMC/CS films matrices (Fig. 3g).

(Fig. 4) shows the FTIR spectra of WPNCC, HPMC/CS neat film and their bio nanocomposite film. The infrared spectra of HPMC/CS film indicate the broad vibration bands at 3200-3400 cm^{-1} due to O-H stretching (H-bonding), at 2910 cm^{-1} for stretching of C-H branch related to CH_2 groups of glucose units in the HPMC and CS. The vibration at 1162 cm^{-1} is for C-O stretching. Absorbance at 1637 cm^{-1}, is

attributed to water molecules adsorption in HPMC and CS. The vibration at 1404 cm^{-1} is for C-N stretching because of adhesion of the cationic groups to the CS [48]. For cellulose nanocrystals, the peaks at 3365 cm^{-1} for O–H stretch band is because of vibrations of the hydrogen bonded hydroxyl (OH) group [49]. The peaks at 2906 cm^{-1} are because of the stretching vibration of aliphatic saturated C–H in cellulose. The cellulose hydrophilic propensity is reflected in the wide absorption band in the 3100– 3500 cm^{-1} area that is relevant to the existence of –OH groups in their main parts. The peak at 1640 cm^{-1} can be owing to the bending mode of the absorbed water and presence of carboxylate groups [49]. The peaks vibrations at 1425 cm^{-1} and 2906 cm^{-1} are owing to C–H metamorphosis (asymmetric) and aliphatic compounds of nanocrystals and demonstrates the crystallinity of cellulose [50]. The peak at 1314 cm^{-1} shows CH_2 shaking vibration in cellulose. The peak at 1160 cm^{-1} is because of C–O–C asymmetric stretch vibration in cellulose. In nanocomposite films the vibration at 1427 cm^{-1} corresponds to CH_2 bending vibration which is ascribed to the cellulose crystalline peak. The peak at 1160 cm^{-1} corresponds to the asymmetric ring breathing mode of cellulose while the band at 1055 cm^{-1} corresponds to the C–OH bending vibrations of alcohol groups present in cellulose [51].These additional bands along with the characteristic peaks of HPMC/CS confirmed the presence of WPNCC in the nanocomposite films. The peaks between 1000 cm^{-1} and 1100 cm^{-1} in nanocomposites are because of the vibration and stretching of C-O and C-C groups of WPNCC. As can be seen in (Fig. 4) by the addition of WPNCC into HPMC/CS matrix, the hydrogen bonding pattern of HPMC/CS also changed as evidenced from the spectra. The broad band in WPNCC (3365 cm^{-1}) was shifted to a lower wave length in nanocomposites (3350- 335 cm^{-1}) which suggests that the addition of WPNCC enhanced the concentration of strongly hydrogen bonded hydroxyl groups in the HPMC/CS matrix or in other words strong inter molecular interactions through hydrogen bonding were existing between WPNCC and HPMC/CS (-OH groups on the surface of nanocrystals interacting with adjacent -OH groups in the HPMC/CS) [52, 53]. Similar results were reported earlier, where the absorption band of OH groups of HPMC at 3448 cm^{-1} was shifted to a lower wave number of 3305 cm^{-1} when nanogels with poly acrylic acid were formed [54]. The cluster of absorptions at 1369, 1334, and 1252 cm^{-1} can be attributed to the bending of CH, CH_2, and OH of nanocrystals, which are typical characteristics of polysaccharide components. Other bands at 1160, 1637, and 1055 cm^{-1} held their intensity after WPNCC addition. These bands are attributed to typical cellulosic compounds and are assigned to C-O, C=O, C-C, and ring structures, in addition to external deformational vibrations of C-H, C-OH, C-CO, and C-CH groups, as already mentioned by [55]. These types of interactions can also contribute to the improved mechanical properties of nanocomposites [56].

The optical absorption, transparency and local dispersion of WPNCC for HPMC/CS film and its bio-nanocomposite films were studied by UV–vis absorption. The UV–Vis spectra of such films are presented in (Fig. 5). Evidently, the neat polymer film is transparent in the UV–Vis region, resulting in a very low absorption level and high transparency as shown in (Fig. 6), indicating that HPMC and CS were well blended because of their high compatibility [57]. Furthermore, when WPNCC were added to the PVA/CS polymer blend, all the investigated bio-nanocomposite films maintained the same absorption level of the HPMC/CS polymer blend. This observation confirmed that the clarity of HPMC/CS was not affected by

the addition of WPCNC, as visually observed for the as-prepared films (Fig. 6), Because the WPNCC are smaller than the wavelength of visual light [58] the UV–Vis results of bionanocomposite films confirmed that the WPNCC were dispersed/distributed in nanoscale within the HPMC/CS matrix. This is directly related to strong interfacial interactions between the macromolecular chains of polymers and the surface of WPNCC, as evidenced by FTIR measurements [58].

3.3. Water vapor permeability

WVP is related to the facility or difficulty of water vapor molecules diffuse across the micro pathways of the composite network microstructure. This diffusion could be affected by the amount of OH groups, insoluble agglomerates and particles dispersed in the microstructure [59]. (Fig. 7a) indicates the effect of WPNCC incorporation on the water vapor permeability of the HPMC/CS nanocomposites. The rate of WVP reduced with increment of WPNCC contents. For all nanocomposites incorporated with WPNCC, the lower WVP values were obtained in comparison with neat HPMCCS film. WVP of the neat sample was 8.22 g Mm m^{-2} day kPa that shows the relatively poor barrier property against water vapor in plasticized HPMC/CS film. However, this value is lower than reported for neat CS film (8.31 g Mm m^{-2} day kPa) [27] and for neat HPMC film (9.64 g Mm m^{-2} day kPa) [60]. It can be concluded that incorporation of HPMC and CS can make lower WVP values because of their strong interaction and electrostatic bonding made by CS. The WVP values of the nanocomposites were reduced by increasing the WPNCC contents and the lower value was seen in the nanocomposite with 9% WPNCC (5.13 g Mm m^{-2} day kPa). Water vapor passes from the amorphous districts of biopolymer; hence the crystallinity degree is important in the vapor permeance of the film [9]. Other researchers informed that loading of 10 wt. % of NCC into the mango puree-based nanocomposites was efficient for remarkable reduction in WVP. That was also showed that with addition of 10 wt% of NCC, permeability of mango puree-based nanocomposites was ameliorated 24% in comparison with pure film [27]. The increase in water vapor barrier property of HPMC/CS/WPNCC nanocomposite films is mainly attributed to the tortuous path for water vapor diffusion due to the impermeable nanocrystals distributed in the polymer matrix increases the effective diffusion path length. In fact, the existence of WPNCC enhances the tortuosity in the CS based nanocomposites which is caused to slower dispersion processes and consequently to lower permeability. With less permeability of the nanoparticle and its well dispersion within the matrix, the barrier properties will enhance [26]. Presence of WPNCC probably modified the micro-pathways of the HPMC/CS matrix, the large number of OH groups that compose the HPMC chains provides strong interactions between water molecules and matrix. Homogenous dispersion and high concentration of WPNCC in HPMC/CS matrix and strong electrostatic bonds made by CS, increased the number of interactions between them, which modified the film structure micro-pathways. The hydrophobic characteristic of WPNCC can decrease the number of water-polymer interactions and consequently decrease the WVP of the HPMC/CS/WPNCC nanocomposite films [59].

3.4. Films solubility

The water solubility of the HPMC/CS bio nanocomposites with various content of WPNCC is shown in (Fig. 7b). The solubility of neat HPMC/CS film in water was 29.46%. With addition of 3 wt% WPNCC in to the HPMC/CS matrix, solubility reduced to 25.54%. With increasing the amounts of WPNCC, the solubility of the nanocomposites was decreased and the lowest solubility value was seen in the nanocomposite comprised 9% WPNCC (17.27%). As can be seen, the effect of WPNCC on the water solubility of the films was considerable. The hydroxyl groups of WPNCC can make strong hydrogen bonds with the hydroxyl groups of HPMC and CS, so improving the interactions between the molecules, can improve the coherence of biopolymer matrix and diminish the water sensitivity [27]. WPNCC nanoparticles are able to interact with HPMC and CS chains through hydrogen bonds with their hydroxyl groups and CS can make strong electrostatic bonds with HPMC and WPNCC because of its surface positive charges. Previous researches showed that the decrease was seen in samples solubility incorporated with various nanoparticles is usually relevant to the formation of strong hydrogen bond between hydroxyl groups of the nanofillers and biopolymer [61]. Also, the other researchers reported that these interactions ameliorate the cohesiveness of the polymer and diminish the sensitivity to water because water molecules can't break these strong bonds [62]. Furthermore, Water uptake of the nanocomposite films depends on the nature of the matrix and filler. This phenomenon of decreased water uptake can be ascribed to the fact that highly crystalline WPNCC is less hydrophilic than HPMC and CS and the formation of strong filler-matrix interactions. In the current study, the cellulose nanocrystals acted as an interpenetrated network within the matrix and prevented the swelling of the HPMC/CS films when exposed to water. Other researchers have also reported similar decrease in water solublity of the nanocomposite films due to the addition of cellulose nanocrystals [63].

3.5. Moisture absorption

The moisture absorption of the HPMC/CS based films is shown in (Fig. 7c). This characteristic decreased with loading of WPNCC owing to the hydrogen bonds formation between HPMC, CS, and WPNCC. It causes that free molecules of water do not interact as forcefully as with HPMC/CS nanocomposites as with HPMC/CS sample lonely [64]. The neat HPMC/CS film had the moisture absorption of 28% in 58% relative humidity at 25 ^{o}C. It is seen that by addition of 3 wt% WPNCC into the HPMC/CS matrix, the moisture absorption decreased to 26%. With increasing the amounts of WPNCC, the moisture absorption of the samples decreased. The lowest value of moisture absorption was seen in the sample with 7% WPNCC and after addition of 9% and 11% WPNCC, the moisture absorption of the films increased. It must be noticed that WPNCC was prepared by removing part of the amorphous regions, leaving the less accessible crystalline region as fine crystals, which are not involved in binding water molecules (since they are mostly impermeable). On the other hand, cellulose nanocrystals partially "blocks" hydrophilic sites of HPMC and CS by hydrogen bonds with OH groups, leaving less OH groups to interact with water molecules, resulting in lower moisture absorption values. However, by adding higher WPNCC contents (9 and 11 wt%), an increase of moisture absorption was observed, which was attributed to filler aggregation, leaving in consequence relatively less surface area per crystal volume to interact with polymer matrix. Similar results were found in the literature: a higher resistance of thermoplastic starch to water was reported when increasing the cellulose nanoparticle content [63], which was ascribed to the presence of

strong hydrogen bonding interactions between particles and between the starch matrix and NCC. These authors also suggested that hydrogen bonding interactions in the composites tend to stabilize the starch matrix when they were submitted to highly moist atmosphere and also that the high crystallinity of cellulose could be responsible for the decreased water absorption [65].

3.6. Oxygen permeability

Oxygen can cause oxidation which is an initial stage of several forms of food deterioration. A film that acts as a proper oxygen barrier can help to improve food quality and extend food shelf life. The oxygen permeability coefficient (OPC) of the HPMC/CS based films is shown in (Fig. 7d). The neat CS or HPMC films separately present poor oxygen barrier properties for packaging applications which further diminish due to the presence of plasticizers. In this study it can be seen that the neat blended HPMC/CS film had the OPC of 41 cm^3 m^{-2} day^{-1}.Pa^{-1} and with addition of only 3 wt% WPNCC into the HPMC/CS matrix, the OPC decreased to 34 cm^3 m^{-2} day^{-1}.Pa^{-1}. With increasing the amounts of WPNCC, the OPC of the samples was decreased and the lowest value of OPC was seen in the sample with 9% WPNCC (17 cm^3 m^{-2} day^{-1}.Pa^{-1}). The reduction in OPC of the nanocomposites owing to which creates a more tortuous path for the permeation of oxygen molecules presence of WPNCC diffused phase in the HPMC/CS film matrix. NCC are perceived to enhance the gas barrier properties by making a maze or “tortuous path” that delays the progress of gas molecules through the matrix [66]. The mechanism for the improvement is ascribed to the enhancement in the tortuosity of the diffusive path for an infiltrating molecule. In fact, the molecules must travel through the substance will have an effect on the barrier properties of the substance [67]. Homogeneous distribution of WPNCC nanoparticles in the polymer matrix and Strong interactions between HPMC and CS chains and WPNCC in the matrix of polymer have efficient roles in barrier properties improvement and substantial decrease of OPC and decrease the diffusivity by decrease of hollows in the biopolymer matrix.

3.7. Mechanical properties of nanocomposites

The reinforcement effect of the different contents of WPNCC on the mechanical properties of the HPMC/CS nanocomposites films was evaluated up to their failure. The tensile strength (TS) and the elongation at break (EB) of the nanocomposite films are shown in (Fig. 8). As can be seen, the TS of the neat HPMC/CS film is improved from 5.13 MPa to 6.92 MPa by addition of only 3 wt% WPNCC, which means the TS is enhanced by 35%. It must be noticed that the TS value of the neat blended HPMC/CS film was higher than reported by other researchers for neat HPMC film (4.2 Mpa) and neat CS film (4.1 Mpa), and it confirms the effectiveness of combination of these polymer together, resulting high TS value than separate usage [27, 59].With increasing the amounts of WPNCC, the TS values of the nanocomposite films increased and the higher TS value was seen in the sample contained 9 wt% WPNCC (8.21 Mpa), which means the TS is increased by 60% compared to the neat HPMC/CS film. NCC played a reinforcing role in HPMC/CS matrix hence, it makes higher TS values for HPMC/CS based nanocomposites. The increase in the TS values of the WPNCC-reinforced HPMC/CS films can be attributed to two factors such as, (1) the favorable nanocrystal–polymer interactions and (2) the reinforcing effect occurred through effective stress transfer at the nanocrystal–polymer interface [68].

Also, the improvement in TS can be owing to the good interfacial interaction between WPNCC, HPMC and CS. It's because of the analogous structures of starch and cellulose and also due to the interactions between the anionic surface charge of the WPNCC and HPMC with the cationic surface charge of CS could make a good interface between the nanoparticle and biopolymer matrix. It can result high tensile strength values for the bio nanocomposites. Also, a mean field mechanical model may be adopted to explain the reinforcing effect of WPNCC observed in this study. The mean-field model is based on the concept that the nanocrystals are homogeneously dispersed in the polymer matrix, but there is no interaction between the nanocrystals [68]. The high mechanical strength of the nanocomposite films may results from efficient load transfer to the nanocrystal network, leading to more uniform stress distribution and minimization of the stress concentration area [69]. Similarly, Chang et al, confirmed the improving property of NCC with thermoplastic starch nanocomposites [70]. On the other hand, at higher content of WPNCC (11 wt%), the improvement isn't as much as in 9 wt% concentration and it is maybe due to the WPNCC agglomeration in the film samples. Preda et al, concluded that applying of 12 wt% NCC does not aid to further improvement of TS [65]. This can be related to the aggregation of NCC particles above a certain concentration, which causes no further improvement of mechanical properties. The elongation at break (EB) of the HPMC/CS neat film was reduced with loading of WPNCC. It was decreased from 23–19% with loading of 3 wt% WPNCC. A significant decrease down to 13% in the EB value of the films was seen in the sample contained 11 wt% WPNCC. Nanocomposites with 11% WPNCC, which indicates a relative reduction of 43% compared to the neat sample. Such a decrease in EB values indicated that the incorporation of WPNCC into the HPMC/CS matrix resulted in strong interactions between filler and matrix, which restricted the motion of the matrix and hence decreased EB [66]. Other researchers informed that elongations at break decreased by loading of NCC in thermoplastic starch films [70]. In comparison to EB and TS values of the low density polyethylene (LDPE; EB=100–650%; TS=8.3–31.4 MPa), HPMC/CS nanocomposite films exhibited good and almost comparable TS values as a biopolymer [71]. HPMC/CS nanocomposite films showed lower elasticity and high stiffness than LDPE. So, it can be inferred that the HPMC/CS/WPNCC9% nanocomposite is a good combination for achieving high improvement in mechanical properties of nanocomposites.

3.8. Disintegrability in composting of HPMC/CS film and its nanocomposites

One of the important properties of the polymers in great applications like food packaging, is biodegradation in compost to restrict the critical problems of waste disposal. Many studies have been done on the effect of nanofillers on some biopolymers biodegradation in last few years and several deferments in biodegradability of the polymer was seen [72]. That is because of the improvement in water barrier properties of the bio nanocomposites, which could prevent the water distribution through the bulk regions and eventually diminish the rate of hydrolysis [73]. The investigation of the decomposition in composting status of HPMC/CS bio nanocomposites was performed to appraise the effect of loading of WPNCC nanofiller on the degradability properties of the HPMC/CS film. (Fig. 9) indicates the progress in disintegrability rates at various times of incubation. After day first, deformation of nanocomposites surface was observed for all substances and after three days these changes were increased in

composting status. These observations showed the start of the hydrolytic decomposition. The transparency losing was seen for all nanocomposites might be ascribed to shifts in the refractive index owing to the absorption of water and forming the compounds with low molecular weight after the hydrolytic degradation [72]. It has been shown that the HPMC/CS film hydrolysis starts in the amorphous area of the biopolymer and consequently changes the crystallinity of the biopolymer. At 6th day, weight loss and fragmentation of the films were seen for all specimens except for neat HPMC/CS film, which its fragmentation began after day 9th. That was also seen that after 23 days in composting status, the nanocomposite samples with WPNCC gained disintegration of 90%. Incorporation of WPNCC enhanced the degradation velocity of HPMC/CS based films gaining 67% at 10 days for sample with 11 wt% WPNCC compare to 42% for the pure CS film. It might be due to the double effect caused with loading of a hydrophilic cellulose nanoparticles, which are anticipated to speed up the disintegration rate of the HPMC/CS films. However, NCC could also restrict the water distribution with enhance the barrier properties and eventually postponing hydrolysis and further decomposition. It can be concluded that all these investigated samples began the disintegration procedure before HPMC/CS neat sample and with higher values, offering their perspective benefits for industrial applications, which need to short degradation time.

4. Conclusions

In this study the production of cellulose nanocrystals was successfully done by HCl hydrolysis after alkali treatment and deinking of fibers. Also, the HPMC/CS nanocomposites were made by solvent casting method. The cellulose nanocrystals were successfully made from waste papers with hydrolysis yield of 65% and high crystallinity index of 79.6%. The rod like WPNCC particles had an average diameter and length of 22± 7 nm and 125± 25 nm, respectively. X-ray diffraction results confirmed the successfully production of cellulose nanocrystals from waste papers and effective presence of these nanoparticles in the HPMC/CS matrix. The FTIR test showed the forming of new hydrogen bonds between the polymers hydroxyl groups and nanoparticles. FESEM analysis proved that the dispersion of WPNCC in the polymer matrix was homogenous, except at high concentration of WPNCC (11 wt%). The optical clarity of HPMC/CS based films was almost unaffected in presence of WPNCC. Based on our results the nanocomposites showed the highest barrier, mechanical and biodegradablility properties with addition of WPNCC and the optimum value of WPNCC was obtained at 9 wt%. It can prove that these nanocomposites present excellent potential as a new biomaterial for application in food packaging and conservation.

Declarations

Acknowledgment

The authors would like to thank the sari agricultural sciences and natural resources university (SANRU) for supplying the equipment of this research project with No. 04-1399-03.

Data availability statement

Authors can confirm that all data supporting the findings of this study are included in the article.

Declaration of interest

The authors declare that they have no known competing financial interests or personal relationships that could have appeared to influence the work reported in this paper.

References

1. Alliot, M.L., Avila, A.T., Argentina, A.: Destintado de papel por flotación: influencia de los factores de forma. AIDIS Argentina. Desafíos ambientales y del saneamiento en el siglo XXI. AIDIS Argentina, Buenos Aires (2004)
2. Joshi, G., Naithani, S., Varshney, V.K., Bisht, S.S., Rana, V.: Potential use of waste paper for the synthesis of cyanoethyl cellulose: A cleaner production approach towards sustainable environment management. J. Clean. Prod. **142**, 3759–3768 (2017)
3. Su, H., Zhu, P., Zhang, L., Zhou, F., Li, G., Li, T., Wang, Q., Sun, R., Wong, C.: Waste to wealth: A sustainable and flexible supercapacitor based on office waste paper electrodes. J. Electroanal. Chem. **786**, 28–34 (2017)
4. Joshi, G., Naithani, S., Varshney, V.K., Bisht, S.S., Rana, V., Gupta, P.K.: Synthesis and characterization of carboxymethyl cellulose from office waste paper: A greener approach towards waste management. J. Waste. Manag. **38**, 33–40 (2015)
5. Delgado-Aguilar, M., Tarres, Q., Pelach, M.A., Mutje, P., Fullana-i-Palmer, P.: Are Cellulose Nanofibers a Solution for a More Circular Economy of Paper Products? Environ. Sci. Tech. **49**, 12206–12213 (2015)
6. Moon, R.J., Martini, A., Nairn, J., Simonsen, J., Youngblood, J.: Cellulose nanomaterials review: Structure, properties and nanocomposites. Chem. Soc. Rev. **40**, 3941–3994 (2011)
7. Klemm, D., Kramer, F., Moritz, S., Lindström, T., Ankerfors, M., Gray, D., Dorris, A., Nanocelluloses: A new family of nature-based materials, Angew. Chem. Int. Ed. 50, 5438–5466: (2011)
8. Lin, N., Huang, J., Dufresne, A.: Preparation, properties and applications of polysaccharide nanocrystals in advanced functional nanomaterials: A review. Nanoscale **4**, 3274–3294 (2012)
9. Vaezi., K., Asadpour, G., Sharifi, S.H.: Effect of coating with novel bio nanocomposites of cationic starch/cellulose nanocrystals on the fundamental properties of the packaging paper. Polym. Test. **80**, 106080 (2019)
10. Azizi Samir, M.A.S., Alloin, F., Gorecki, W., Sanchez, J.Y., Dufresne, A.: Nanocomposite polymer electrolytes based on poly (oxyethylene) and cellulose nanocrystals. J. Phys. Chem. B. **108**, 10845–10852 (2004)
11. Heath, L., Thielemans, W.: Cellulose nanowhisker aerogels. Green Chem. **12**, 1448–1453 (2010)

12. Paralikar, S.A., Simonsen, J., Lombardi, J.: Poly (vinyl alcohol)/cellulose nanocrystal barrier membranes. J. Membr. Sci. **320**, 248–258 (2008)
13. Wang, H., Roman, M.: Formation and properties of chitosan – cellulose nanocrystal polyelectrolyte – macro ion complexes for drug delivery applications. Biomacromol **12**, 1585–1593 (2011)
14. Peresin, M.S., Habibi, Y., Zoppe, J.O., Pawlak, J.J., Rojas, O.J.: Nanofiber composites of polyvinyl alcohol and cellulose nanocrystals: Manufacture and characterization. Biomacromolecules. **11**, 674–681 (2010)
15. Roman, M., Winter, W.T.: Effect of sulfate groups from sulfuric acid hydrolysis on the thermal degradation behavior of bacterial cellulose. Biomacromolecules. **5**, 1671–1677 (2004)
16. Dong, H., Strawhecker, K.F., Snyder, J.F., Orlicki, J.A., Reiner, R.S., Rudie, A.W.: Cellulose nanocrystals as a reinforcing material for electrospun poly(methyl methacrylate) fibers: Formation, properties and nanomechanical characterization. Carbohydr. Polym. **87**, 2488–2495 (2012)
17. Sheltami, R.M., Abdullah, I., Ahmad, I., Dufresne, A., Kargarzadeh, H.: Extraction of cellulose nanocrystals from mengkuang leaves (pandanus tectorius). Carbohydr. Polym. **88**, 772–779 (2012)
18. Uddin, A.J., Araki, Y., Gotoh, Y.: Characterization of the poly (vinyl alcohol)/cellulose whisker gel spun fibers. Compos. Part A Appl. Sci. Manuf. **42**, 741–747 (2011)
19. Zhang, K., Sun, P., Liu, H., Shang, S., Song, J., Wang, D.: Extraction and comparison of carboxylated cellulose nanocrystals from bleached sugarcane bagasse pulp using two different oxidation methods. Carbohydr. polym **138**, 237–243 (2016)
20. Rohaizu, R., Wanrosli, W.D.: Sono-assisted TEMPO oxidation of oil palm lignocellulosic biomass for isolation of nanocrystalline cellulose. Ultrason. sonochem. **34**, 631–639 (2017)
21. Xu, Y., Kim, K., Hanna, M.A., Nag, D.: Chitosan-starch composite film: Preparation and characterization. Ind. Crops. Prod. **21**, 185–192 (2005)
22. Bhattacharya, M.: Stress relaxation of starch/synthetic polymer blends. J. Mater. Sci. **33**, 4131–4139 (1998)
23. Tang, X., Alavi, S.: Structure and physical properties of starch/poly vinyl alcohol/laponite RD nanocomposite films. J. agric. food. chem. **60**, 1954–1962 (2012)
24. Vaezi, K., Asadpour, G., Sharifi, H.: Effect of ZnO nanoparticles on the mechanical, barrier and optical properties of thermoplastic cationic starch/montmorillonite biodegradable films. Int. j. biol. macromol. **124**, 519–529 (2019)
25. Simkovic, I., Laszlo, J.A., Thompson, A.R.: Preparation of a weakly basic ion exchange by crosslinking starch with epichlorohydrin in the presence of NH4OH, Carbohydr. Polym. **30**, 25–30 (1996)
26. Bilbao-Sainz, C., Bras, J., Williams, T., Sénechal, T., Orts, W.: HPMC reinforced with different cellulose nano-particles. Carbohydr. polym. **86**, 1549–1557 (2011)
27. Vaezi, K., Asadpour, G., Sharifi, S.H.: Bio nanocomposites based on cationic starch reinforced with montmorillonite and cellulose nanocrystals: Fundamental properties and biodegradability study. Int.

J. Biol. Macromol. **146**, 374–386 (2020)

28. Eriksson, M., Pettersson, G., Wågberg, L.: Application of polymeric multilayers of starch onto wood fibres to enhance strength properties of paper. Nord. Pulp. Pap. Res. J. **20**, 270–275 (2005)
29. Hamzeh, Y., Sabbaghi, S., Ashori, A., Abdulkhani, A., Soltani, F.: Improving wet and dry strength properties of recycled old corrugated carton (OCC) pulp using various polymers. Carbohydr. Polym. **94**, 577–583 (2013)
30. Kasiri, N., Fathi, M.: Production of cellulose nanocrystals from pistachio shells and their application for stabilizing Pickering emulsions. Int. J. Biol. Macromol. **106**, 1023–1031 (2018)
31. Segal, L., Creely, J.I., Martin, A.E., Conrad, C.M.: An Empirical Method for Estimating the Degree of Crystallinity of Native Cellulose Using the X-Ray Diffractometer. Tex. Res. J. **29**, 786–794 (1959)
32. Huang, M.F., Yu, J.G., Ma, X.F.: Studies on the properties of montmorillonite-reinforced thermoplastic starch composites. Polymer. **45**, 7017–7023 (2004)
33. Luzi, F., Fortunati, E., Puglia, D., Petrucci, R., Kenny, J.M., Torre, L.: Study of disintegrability in compost and enzymatic degradation of PLA and PLA nanocomposites reinforced with cellulose nanocrystals extracted from Posidonia Oceanica. Polym. Degrad. Stab. **121**, 105–115 (2015)
34. Casillas, R.R., Rodríguez, K.F.B., Cruz-Estrada, R.H., Dávalos-Olivares, F., Navarro-Arzate, F., Satyanarayana, K.G., Isolation and characterization of cellulose nanocrystals created from recycled laser printed paper, BioResources. 2018; 13: 7404-7429 (2018)
35. Wang, Q., Zhao, X., Zhu, J.Y.: Kinetics of strong acid hydrolysis of a bleached kraft pulp for producing cellulose nanocrystals (CNCs). Ind. Eng. Chem. Res. **53**, 11007–11014 (2014)
36. Mohamed, M.A., Salleh, W.N.W., Jaafar, J., Asri, S., Ismail, A.F.: Physicochemical properties of "green" nanocrystalline cellulose isolated from recycled newspaper, Rsc. Adv. **5**, 29842–29849 (2015)
37. Wang, Q.Q., Zhu, J.Y., Reiner, R.S., Verrill, S.P., Baxa, U., McNeil, S.E.: Approaching zero cellulose loss in cellulose nanocrystal (CNC) production: recovery and characterization of cellulosic solid residues (CSR) and CNC. Cellulose. **19**, 2033–2047 (2012)
38. Karim, M., Chowdhury, Z.Z., Hamid, S.B.A., Ali, M.: Statistical optimization for acid hydrolysis of microcrystalline cellulose and its physiochemical characterization by using metal ion catalyst. Materials. **7**, 6982–6999 (2014)
39. Lu, H., Gui, Y., Zheng, L., Liu, X.: Morphological, crystalline, thermal and physicochemical properties of cellulose nanocrystals obtained from sweet potato residue. Food. Res. int. **50**, 121–128 (2013)
40. Lei, W., Fang, C., Zhou, X., Yin, Q., Pan, S., Yang, R., Liu, D., Ouyang, Y.: Cellulose nanocrystals obtained from office waste paper and their potential application in PET packing materials. Carbohydr. Polym. **181**, 376–385 (2018)
41. Chen, L., Zhu, J.Y., Baez, C., Kitin, P., Elder, T.: Highly thermal-stable and functional cellulose nanocrystals and nanofibrils produced using fully recyclable organic acids. Green Chem. **18**, 3835–3843 (2016)

42. Wang, Z., Yao, Z., Zhou, J., He, M., Jiang, Q., Li, S., Ma, Y., Liu, M., Luo, S.: Isolation and characterization of cellulose nanocrystals from pueraria root residue. Int. J. Biol. Macromol. **129**, 1081–1089 (2019)
43. De Melo, E.M., Clark, J.H., Matharu, A.S.: The Hy-MASS concept: hydrothermal microwave assisted selective scissoring of cellulose for in situ production of (meso) porous nanocellulose fibrils and crystals. Green Chem. **19**, 3408–3417 (2017)
44. Filson, P.B., Dawson-Andoh, B.E., Schwegler-Berry, D.: Enzymatic-mediated production of cellulose nanocrystals from recycled pulp. Green Chem. **11**, 1808–1814 (2009)
45. Neto, W.P.F., Silvério, H.A., Dantas, N.O., Pasquini, D.: Extraction and characterization of cellulose nanocrystals from agro-industrial residue–Soy hulls. Ind. Crops. Prod. **42**, 480–488 (2013)
46. George, J., Kumar, R., Sajeevkumar, V.A., Ramana, K.V., Rajamanickam, R., Abhishek, V., Nadanasabapathy, S.: Hybrid HPMC nanocomposites containing bacterial cellulose nanocrystals and silver nanoparticles. Carbohydr. Polym. **105**, 285–292 (2014)
47. Agustin, M.B., Ahmmad, B., De Leon, E.R.P., Buenaobra, J.L., Salazar, J.R., Hirose, F.: Starch-based biocomposite films reinforced with cellulose nanocrystals from garlic stalks. Polym. Compos. **34**, 1325–1332 (2013)
48. Pal, S., Mal, D., Singh, R.P.: Cationic starch: an effective flocculating agent. Carbohydr. Polym. **59**, 417–423 (2005)
49. Sun, X.F., Xu, F., Sun, R.C., Fowler, P., Baird, M.S.: Characteristics of degraded cellulose obtained from steam-exploded wheat straw. Carbohydr. Res. **340**, 97–106 (2005)
50. Shankar, S., Rhim, J.W.: Preparation of nanocellulose from micro-crystalline cellulose: The effect on the performance and properties of agar-based composite films. Carbohydr. polym. **135**, 18–26 (2016)
51. George, J., Sajeevkumar, V.A., Ramana, K.V., Sabapathy, S.N.: Augmented properties of PVA hybrid nanocomposites containing cellulose nanocrystals and silver nanoparticles. J. Mater. Chem. **22**, 22433–22439 (2012)
52. Leppänen, K., Andersson, S., Torkkeli, M., Knaapila, M., Kotelnikova, N., Serimaa, R.: Structure of cellulose and microcrystalline cellulose from various wood species, cotton and flax studied by X-ray scattering. Cellulose. **16**, 999–1015 (2009)
53. Fortunati, E., Puglia, D., Monti, M., Santulli, C., Maniruzzaman, M., Kenny, J.M.: Cellulose nanocrystals extracted from okra fibers in PVA nanocomposites. J. Appl. Polym. Sci. **128**, 3220–3230 (2013)
54. Yao, R., Xu, J., Lu, X., Deng, S.: Phase transition behaviour of HPMC-AA andpreparation of HPMC-PAA nanogels, J. Nanomater. 6 pages, (2011)
55. Huq, T., Salmieri, S., Khan, A., Khan, R.A., Le Tien, C., Riedl, B., Fraschini, C., Bouchard, J., Uribe-Calderon, J., Kamal, M.R., Lacroix, M.: Nanocrystalline cellulose (NCC) reinforced alginate based biodegradable nanocomposite film. Carbohydr. polym. **90**, 1757–1763 (2012)
56. Dogan, N., McHugh, T.H.: Effects of microcrystalline cellulose on functionalproperties of hydroxy propyl methyl cellulose microcomposite films. J. Food Sci. **72**, 16–22 (2007)

57. Bonilla, J., Fortunati, E.L.E.N.A., Atarés, L., Chiralt, A., Kenny, J.M.: Physical, structural and antimicrobial properties of poly vinyl alcohol–chitosan biodegradable films. Food. Hydrocoll. **35**, 463–470 (2014)
58. El Miri, N., Abdelouahdi, K., Zahouily, M., Fihri, A., Barakat, A., Solhy, A., El Achaby, M.: Bio-nanocomposite films based on cellulose nanocrystals filled polyvinyl alcohol/chitosan polymer blend, J. Appl. Polym. Sci. 132 (22) (2015)
59. De Matos Fonseca, J., Valencia, G.A., Soares, L.S., Dotto, M.E.R., Campos, C.E.M., Moreira, R.D.F.P.M., Fritz, A.R.M.: Hydroxypropyl methylcellulose-TiO2 and gelatin-TiO2 nanocomposite films: Physicochemical and structural properties. Int. J. Biol. Macromol. **151**, 944–956 (2020)
60. Hay, W.T., Fanta, G.F., Peterson, S.C., Thomas, A.J., Utt, K.D., Walsh, K.A., Selling, G.W.: Improved hydroxypropyl methylcellulose (HPMC) films through incorporation of amylose-sodium palmitate inclusion complexes. Carbohydr. Polym. **188**, 76–84 (2018)
61. Rhim, J.W., Ng, P.K.: Natural biopolymer-based nanocomposite films for packaging applications. Crit. Rev. Food. Sci. Nutr. **47**, 411–433 (2007)
62. Tunc, S., Angellier, H., Cahyana, Y., Chalier, P., Gontard, N., Gastaldi, E.: Functional properties of wheat gluten/montmorillonite nanocomposite films processed by casting. J. Membra. Sci. **289**, 159–168 (2007)
63. Svagan, A.J., Hedenqvist, M.S., Berglund, L.: Reduced water vapour sorption in cellulose nanocomposites with starch matrix. Compos. Sci. Technol. **69**, 500–506 (2009)
64. Almasi, H., Ghanbarzadeh, B., Entezami, A.A.: Physicochemical properties of starch–CMC–nanoclay biodegradable films. Int. J. Biol. Macromol. **46**, 1–5 (2010)
65. Pereda, M., Dufresne, A., Aranguren, M.I., Marcovich, N.E.: Polyelectrolyte films based on chitosan/olive oil and reinforced with cellulose nanocrystals. Carbohydr. Polym. **101**, 1018–1026 (2014)
66. Azeredo, H.M., Mattoso, L.H.C., Wood, D., Williams, T.G., Avena-Bustillos, R.J., McHugh, T.H.: Nanocomposite edible films from mango puree reinforced with cellulose nanofibers. J. Food Sci. **74**, 31–35 (2009)
67. Ray, S.S., Okamoto, M.: Polymer/layered silicate nanocomposites: a review from preparation to processing. Prog. Polym. Sci. **28**, 1539–1641 (2003)
68. Khan, A., Khan, R.A., Salmieri, S., Le Tien, C., Riedl, B., Bouchard, J., Lacroix, M.: Mechanical and barrier properties of nanocrystalline cellulose reinforced chitosan based nanocomposite films. Carbohydr. Polym. **90**, 1601–1608 (2012)
69. Kanagaraj, S., Varanda, F.R., Zhil'tsova, T.V., Oliveira, M.S., Simões, J.A.: Mechanical properties of high density polyethylene/carbon nanotube composites. Compos. Sci. Technol. **67**, 3071–3077 (2007)
70. Chang, P.R., Jian, R., Zheng, P., Yu, J., Ma, X.: Preparation and properties of glycerol plasticized-starch (GPS)/cellulose nanoparticle (CN) composites. Carbohydr. Polym. **79**, 301–305 (2010)
71. Callister, W.D.: Materials science and engineering an introduction. John Wiley (2007)

72. Fukushima, K., Tabuani, D., Abbate, C., Arena, M., Ferreri, L.: Effect of sepiolite on the biodegradation of poly (lactic acid) and polycaprolactone. Polym. Degrad. Stab. **95**, 2049–2056 (2010)
73. Lee, S.R., Park, H.M., Lim, H., Kang, T., Li, X., Cho, W.J., Ha, C.S.: Microstructure, tensile properties, and biodegradability of aliphatic polyester/clay nanocomposites. Polymer. **43**, 2495–2500 (2003)

Table 1

Table 1. Source, yield, crystallinity index, and length of the cellulose nanocrystals.

Source	Yield (wt%)	Length (nm)	Crystallinity Index (wt%)	Reference (wt. %)
Office waste papers	65	100-150	79.6	This study
Eucalyptus Kraft pulp Wood	75	275-380	81	[41]
Pueraria root residue	NA*	100-300	60	[42]
Orange peel residues	30-50	200-400	NA	[43]
Recycled pulp	4.9-38	100	NA	[44]
Soy hulls	NA	80-160	73.5	[45]
Pistachio shells	77	50 (spherical)	79.4	[30]

NA* means not reported.

Figures

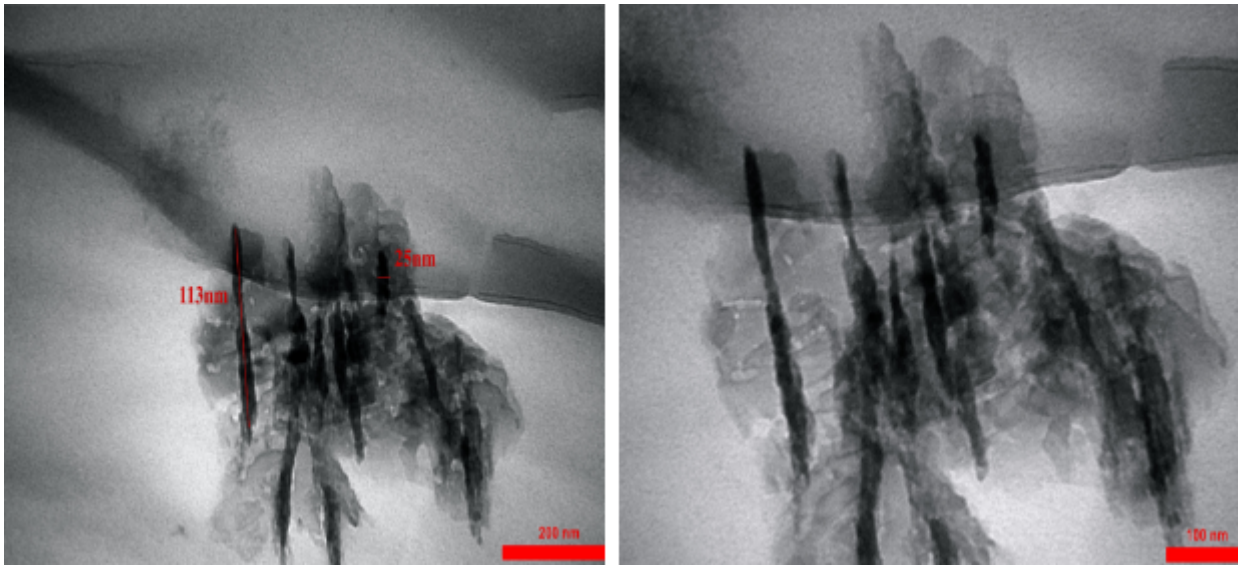

Figure 1

TEM cellulose images of nanocrystals produced from waste papers by HCl hydrolysis.

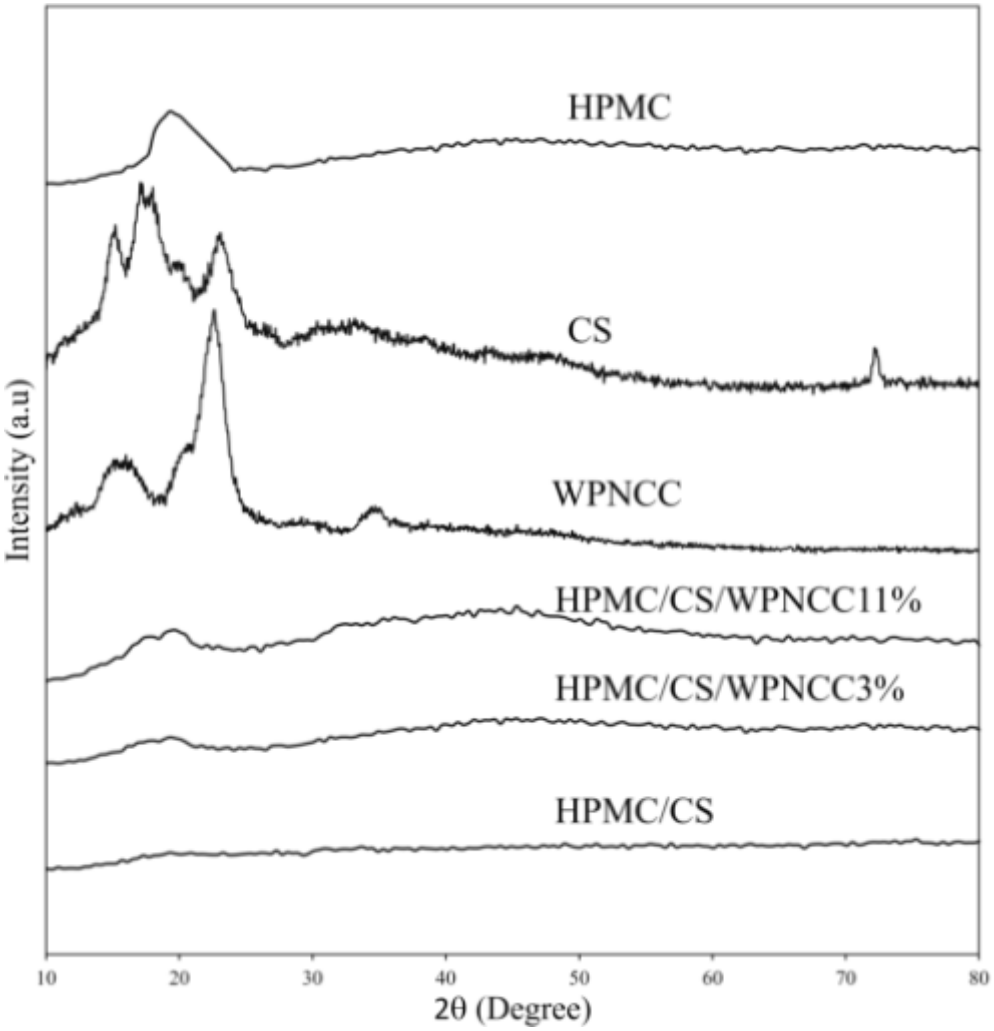

Figure 2

X-ray diffraction of HPMC, CS, WPNCC and their nanocomposite films

Figure 3

FE-SEM images of surface microstructure of HPMC/CS neat film (a) and its nanocomposite films with WPNCC contents of 3 wt% (b), 5 wt% (c), 7 wt% (d), 9 wt% (e), 11 wt% (f), and the nano structure of WPNCC in the films matrices (g).

Figure 4

Infrared spectrum of WPNCC, neat HPMC/CS, and their nanocomposites films.

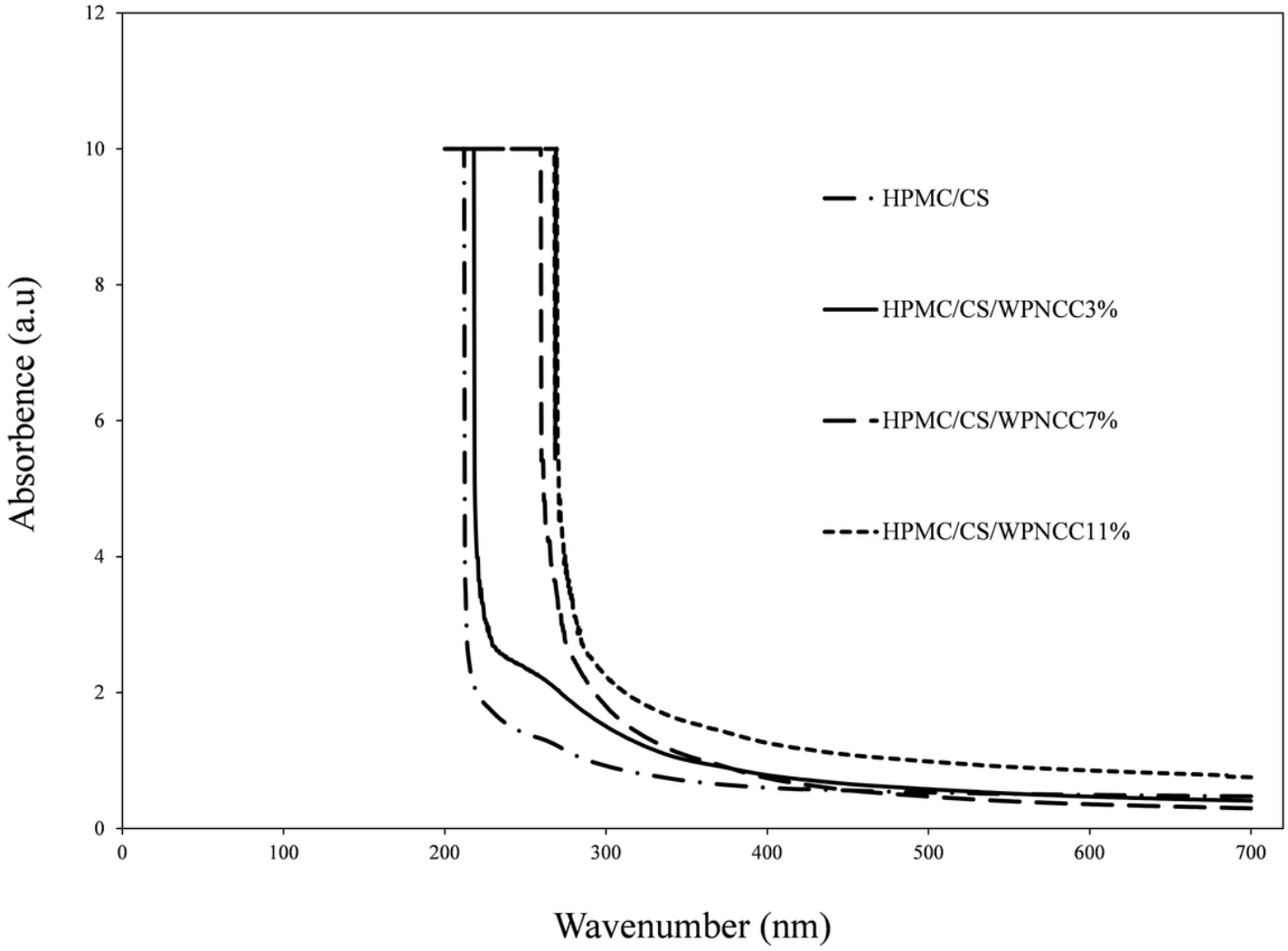

Figure 5

The UV–Vis spectrums of the HPMC/CS film and its nanocomposites with different amounts of WPNCC.

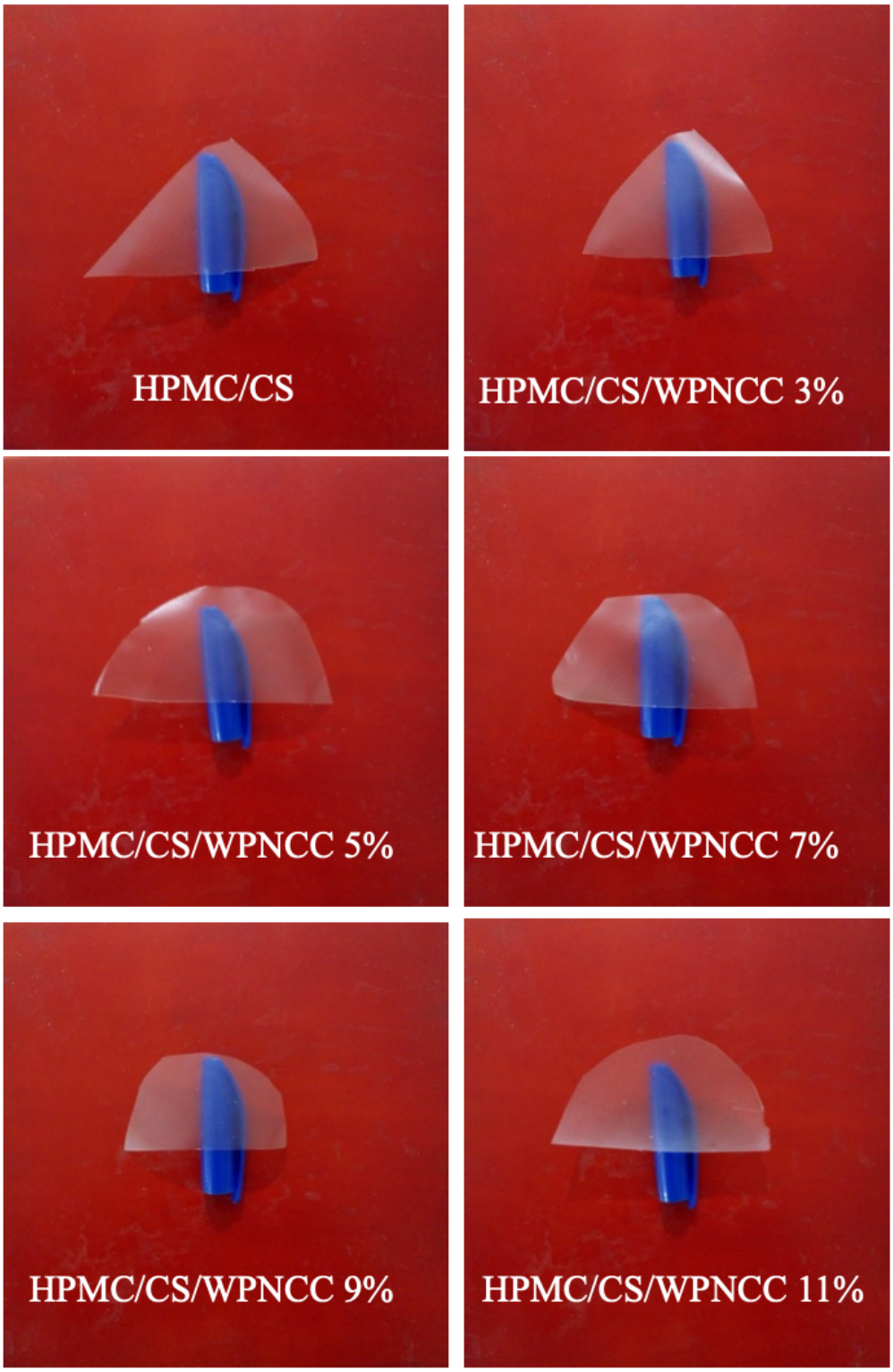

Figure 6

Visual appearance of the HPMC/CS based nanocomposite films with different percentages of WPNCC.

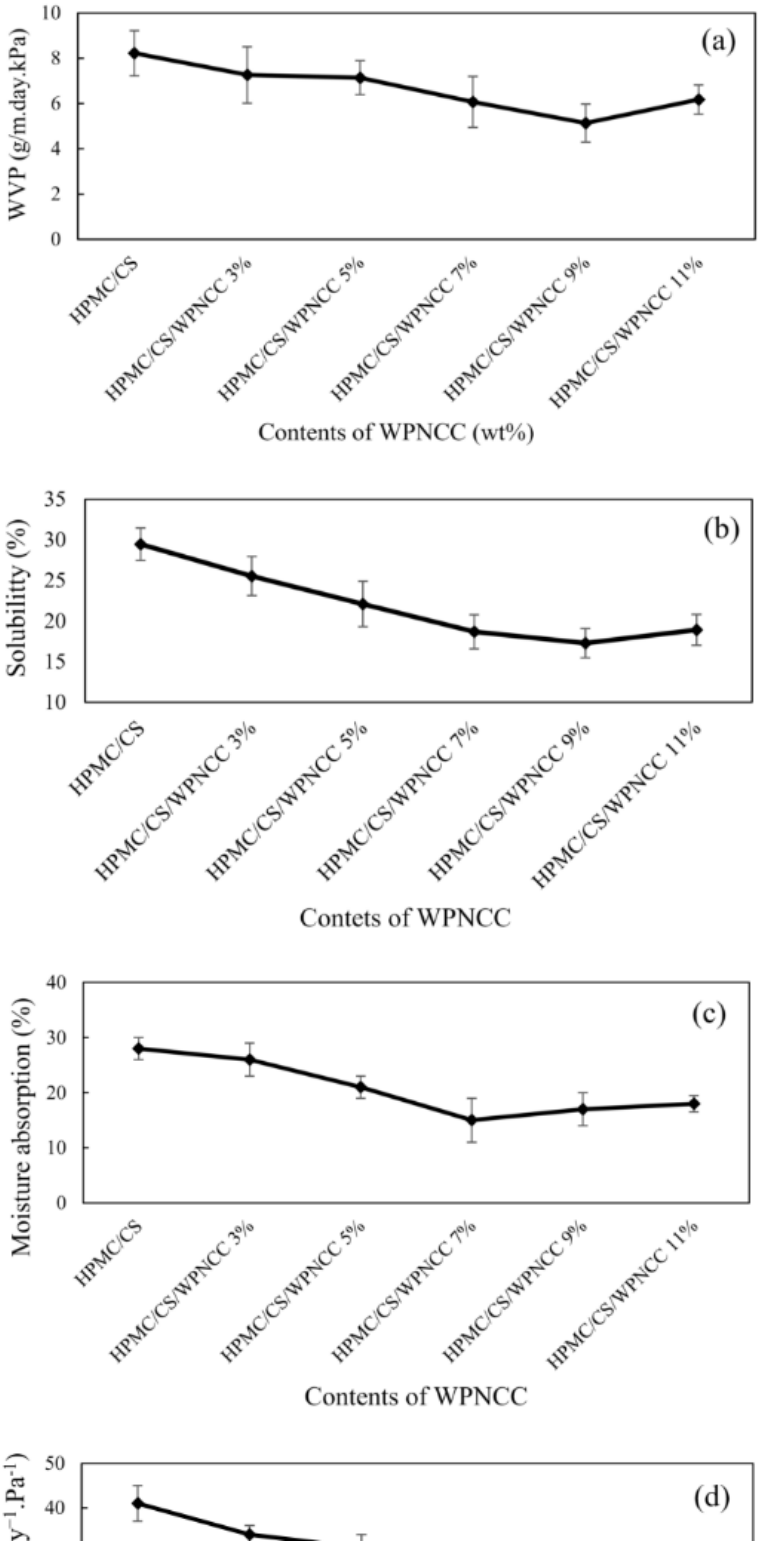

Figure 7

Rate of Water vapor permeability (WVPR) (a), water solubility (b), water absorption (c), and oxygen permeability (d) of the HPMC/CS nanocomposite films and its nanocomposites at various contents of WPNCC.

Figure 8

Effects of WPNCC contents on the tensile strength and elongation at break of the HPMC/CS-based nanocomposite films.

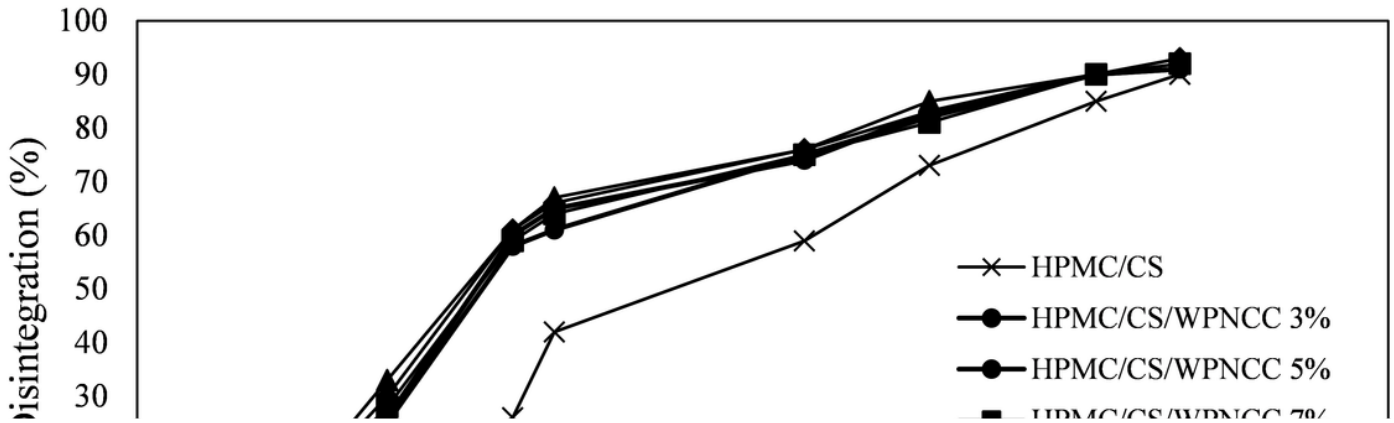

Figure 9

Disintegrability percentage values of HPMC/CS film and its biocomposites contained various amounts of WPNCC at different compost stages of incubation.

Supplementary Files

This is a list of supplementary files associated with this preprint. Click to download.

- supplementaryfile.pdf
- floatimage1.png